Physical and Chemical Investigation of Substrate Temperature Dependence of Zirconium Oxide Films on Si(100)

Misun Chun, Myung-Jun Moon,[†] Juyun Park, and Yong-Cheol Kang[*]

*Department of Chemistry, Pukyong National University, Busan 608-737, Korea. *E-mail: yckang@pknu.ac.kr*
†Department of Industrial Chemistry, Pukyong National University, Busan 606-739, Korea

We report here the surface behavior of zirconium oxide deposited on Si(100) substrate depending on the different substrate temperatures. The zirconium oxide thin films were successfully deposited on the Si(100) surfaces applying radio-frequency (RF) magnetron sputtering process. The obtained zirconium oxide films were characterized by X-ray photoelectron spectroscopy (XPS) for study about the chemical environment of the elements, X-ray diffraction (XRD) for check the crystallinity of the films, spectroscopic ellipsometry (SE) technique for measuring the thickness of the films, and the morphology of the films were investigated by atomic force microscope (AFM). We found that the oxidation states of zirconium were changed from zirconium suboxides ($ZrO_{x,y}$, x,y < 2) (x: higher and y: lower oxidation state of zirconium) to zirconia (ZrO_2), and the surface was smoothed as the substrate temperature increased.

Introduction

Zirconium oxide is one of the technologically important materials characterized by a high melting point, ionic conductivity, optical properties. good thermal insulating characteristics. high hardness, large resistance against oxidation. high refractive index. and broad region of low absorption from the near-UV to the mid-IR.[1,2] The combination of these properties is attractive for wide range of applications which include laser mirrors. broad band interference filters. and ionic conductors.[3,4] Also. zirconium oxide thin film may be used as fuel cells,[5] memory device,[6] heat-resistant materials.[7] optical filters.[8] and sensors.[9]

Advantages of zirconia such as its thermal stability with Si substrate and its high dielectric constant make it one of the most promising gate dielectric candidates for SiO_2. Unfortunately. they suffer from mobility degradation, fixed charge issues.[10] Furthermore. they will crystallize at relatively low temperature. leading to the formation of grain boundaries.[10-12]

Zirconium oxide thin films have been widely deposited by various deposition techniques including electron-beam deposition,[13] chemical vapor deposition (CVD).[14] reactive sputtering,[9] radio frequency. direct current reactive magnetron sputtering.[15] and ion beam sputtering deposition.[16] Most of zirconium oxide films were prepared by reactive sputtering using metal target.[17] Some zirconia films were deposited by radio frequency (RF) sputtering with a zirconia ceramic target.[18]

In the present work. zirconium oxide thin films were deposited on p-type Si(100) wafer by RF plasma sputtering from metallic zirconium target in Ar/O_2 plasma gas which is mixed with same volume ratio. The resulted films were obtained at different substrate temperatures.

Experimental Section

Deposition of zirconium oxide. Zirconium oxide films were deposited on p-type Si(100) wafer substrates by reactive RF magnetron sputtering from a metallic zirconium target with a diameter of 50 mm and a thickness of 3 mm. The Si substrates with native oxide were carefully cleaned by known cleaning process[3] before introducing it into the sputtering chamber. The deposition chamber was evacuated using a roughing pump (RP) and a turbo molecular pump (TMP) to 1.0×10^{-5} Torr of base pressure range. The mixed sputtering gas. Ar (99.99% purity) and O_2 (99.99% purity). was introduced into the deposition chamber separately and controlled by standard mass flow controllers. The zirconium target was cleaned by pre-sputtering with an RF power (13.56 MHz) of 20 W for 1 hr with mixed sputter gas while the substrate was shielded in order to remove the surface contaminants on the zirconium target and stabilize the plasma.

In the present work, sputter deposition was performed at different substrate temperatures with the same RF power of 20 W for 3 hr. The pressure of the sputtering chamber during the RF sputtering process was kept at 45 mTorr as measured by a convectron gauge. During the sputtering. the total gases (Ar : O_2, 1 : 1 volume ratio) flowing flux was kept at 20 sccm. The zirconium oxide films were deposited at different substrate temperatures i.e. room temperature, 373, 473, 573, and 623 K.
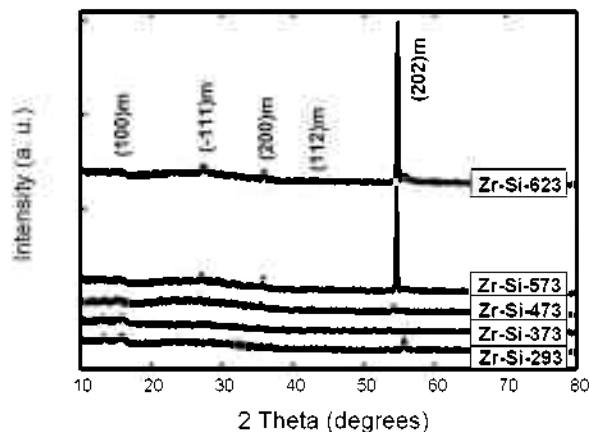
Morphology and thickness of the films. The crystal structure of the zirconium oxide thin films deposited on Si(100) wafer was determined by X-ray diffraction (XRD) using a PHILIPS (Netheland) X'Pert-MPD system applying a grazing mode. The used X-ray source was Cu Kα radiation. The scanning angle, 2θ. was varied from 10° to 80° with a detection step of 0.02°. The JCPDS international diffraction data base[19] has been used to indentify the crystalline phase.

The surface morphology of zirconium oxide film was investigated using an atomic force microscopy (AFM). a Veeco Multimode Digital Instruments Nanoscope IIIα system. in contact mode. The surface roughness was measured as root mean square (RMS) value over the area of 1 μm × 1 μm.
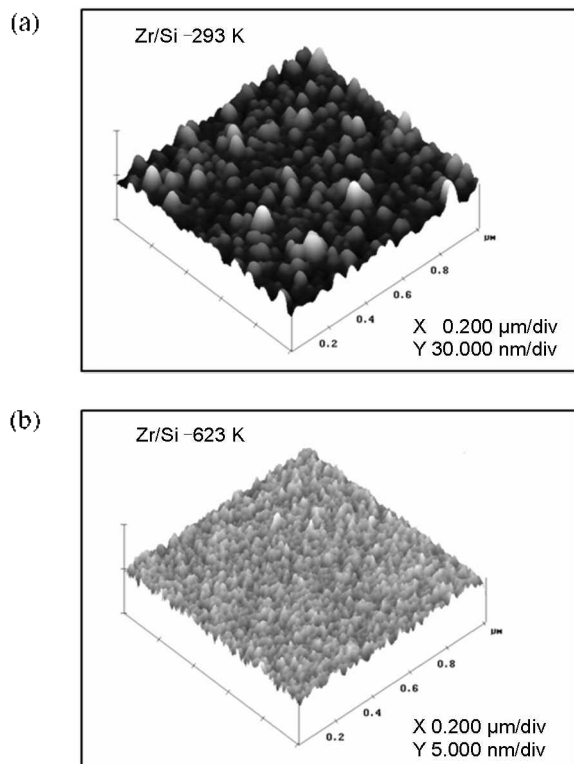
The thickness of the zirconium oxide thin films was deduced by spectroscopic ellipsometry (Gaertner L2W830) (SE). The SE

measurements were performed at incident angles of 70° and a wavelength of 6328 nm. The index of refraction used for zirconium oxide was 2.17 for fitting.

Chemical analysis of the films using XPS. The chemical environment of zirconium oxide thin films was analyzed by XPS (VG ESCALAB 2000), using a monochromatic Al Kα X-ray source (1486.6 eV). The base pressure in the analysis chamber was maintained at about 1×10^{-10} Torr applying with two sets of pumping system and the details were described elsewhere.[20,21]

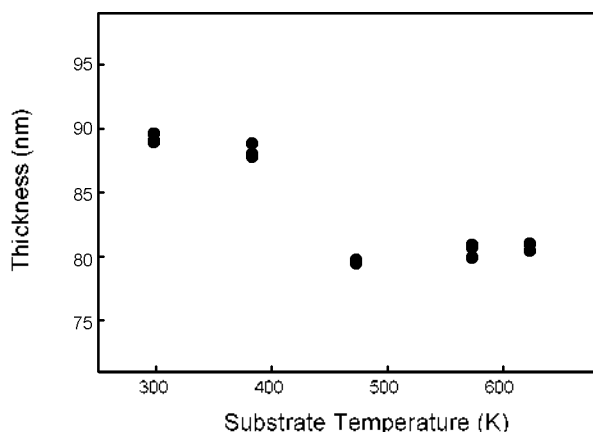The monochromated Al Kα X-ray source was created at a power of 247.5 W. The survey XP spectra were collected in a concentric hemispherical analyzer (CHA) in constant analyzer energy (CAE) mode with pass energy of 50 eV, a dwell time of 50 ms, and an energy step size of 0.5 eV. The binding energy (BE) scale was calibrated by using the peak of adventitious carbon setting it to 284.6 eV.[22] High resolution spectra were obtained at pass energy of 20 eV, an energy step size of 0.05 eV, and other factors were kept the same as those applied in the survey scan.

Results and Discussion

Physical analysis of zirconium oxide thin films. The crystallized structures of the zirconium oxide thin films deposited in various substrate temperatures are shown in Figure 1. It has been reported that zirconia exists in three different crystalline phases. The monoclinic phase is stable up to 1443 K, a tetragonal phase is reported between 1443 and 2643 K, and a cubic phase exists up to the melting point, 3133 K.[23,24] The XRD measurements reveal that the monoclinic phase has formed without any phase mixing. The diffraction peaks were assigned according to standard JCPDS patterns for zirconia (ZrO_2) lattice.[19] Before the Si substrate was heated, the zirconium oxide films showed a very weak diffraction peak for monoclinic $ZrO_2(-111)$ and $ZrO_2(100)$. When the Si substrate was heated over 573 K, there is an increase in the intensity of $ZrO_2(202)$ peak for monoclinic phase. The temperatures applied in this experiment were well below the phase transition temperatures of monoclinic and tetragonal phases of ZrO_2. Only the monoclinic phase of zirconia was observed from the films as expected.

Figure 2 shows the representative AFM images of zirconium oxide thin films deposited on Si(100) at different substrate temperatures taken in contact mode. Figure 2 (a) shows the surface morphology of thin films deposited at room temperature. The roughness of the film was 2.42 nm of RMS. Figure 2 (b) shows the zirconium oxide thin films deposited at 623 K of the substrate temperature and its RMS roughness was 0.23 nm. As the substrate temperature increased, the RMS values are decreased significantly and formed a more regular films surface. Obviously the surface morphology of the film deposited at 623 K is smoother than that of deposited at room temperature. This result could make certain that the roughness of the zirconium oxide thin films decreased by increasing substrate temperature. With increasing the substrate temperature the RMS values decreased, which implies that the substrate temperature has effects on the surface roughness.[25]
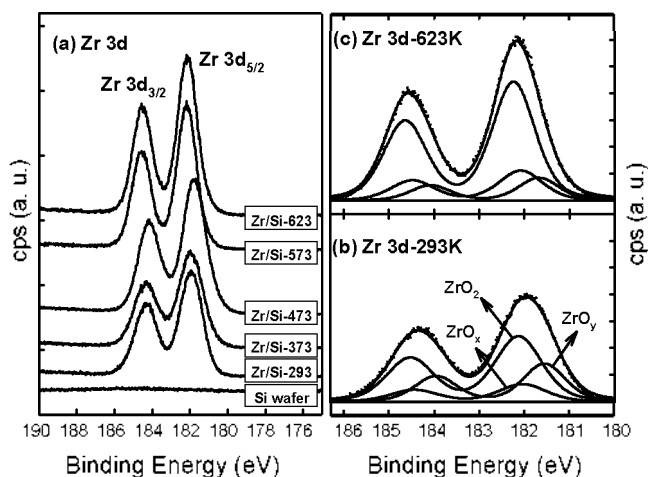
The thickness of zirconium oxide thin films formed at different substrate temperatures deduced by SE technique is shown in Figure 3. The thicknesses of these films were relatively constant about of 85 nm. But, there was a slight decrease in zirconium oxide thin films thickness with the increase of substrate temperature. It may be due to the increased packing density of the surface atoms at high substrate temperature. At high temperature, the deposited atoms have higher mobility and settle down at the thermodynamically stable site and forms monoclinic $ZrO_2(202)$ phase. This result is consistent with the results of XRD experiment.

Figure 1. The XRD patterns of the zirconium oxide thin films deposited on Si(100) with different substrate temperatures in Ar/O₂ plasma ambient. The numbers in the legend box represent substrate temperatures.

Figure 2. AFM images (1 μm × 1 μm) of zirconium oxide thin films on Si(100) with; (a) deposition at room temperature (293 K), (b) deposition and substrate heating at 623 K. Note the scale bars of y-direction: 30 nm/div. for (a) Zr/Si-293 K and 5 nm/div. for (b) Zr/Si-623 K.

Zirconium Oxide Films on Si(100)

Bull. Korean Chem. Soc. **2009**, Vol. 30, No. 11   2731

Figure 3. Thickness of zirconium oxide thin films as a function of substrate temperatures.
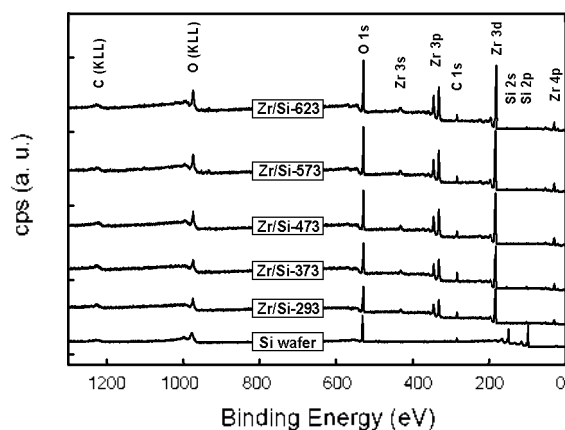
Figure 4. The survey XPS of zirconium oxide on Si(100) before and after zirconium oxide deposition with different substrate temperatures.
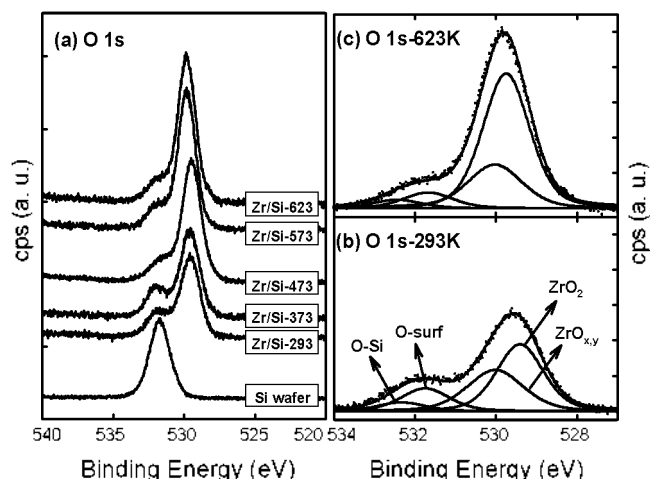

Figure 5. (a) stacked XP spectra of the Zr 3d$_{5/2}$ and 3d$_{3/2}$ of zirconium oxide thin films on Si(100) with increased substrate temperature. Deconvoluted XP spectra of the Zr 3d at the silicon substrate temperature of 293 K (b) and 623 K (c). The Zr 3d spectrum was decomposed three oxidation states; zirconia (ZrO$_2$), zirconium with higher (ZrO$_x$) and lower oxidation states (ZrO$_y$). The dots represent raw data, smooth lines overlapped with the dots represent reconstructed data of deconvoluted Zr 3d components.

X-ray photoelectron spectroscopy. Figure 4 shows the survey XP spectra of zirconium oxide thin films on Si(100) wafer in the binding energy range of 0 ~ 1300 eV. The bottom spectrum was taken from pure silicon wafer. Before zirconium deposition, the Si peaks were detected at 150.5 and 99.5 eV assigned for Si 2s and Si 2p. respectively.[26,27] After zirconium oxide deposition at different substrate temperatures, the XP spectra showed zirconium features that Zr 3s (432.4 eV), Zr 3d (182.0. 184.4 eV). Zr 3p (346, 322 eV). and Zr 4p (30.8 eV).[28,29] The C 1s peak of adventitious carbon presented at 284.6 eV for all films including bare Si wafer.[22] Auger peaks for O (KLL) and C (KLL) were also detected at high binding energy region.[30] The peak intensity of Zr 3d was increased with increasing substrate temperature during zirconium oxide deposition. Also, the peak intensity of O 1s was increased as well. It is clear that zirconium oxide films were coated on the silicon substrate.

The Zr 3d core level XP spectra are shown in Figure 5 (a). Before the Si substrate was heated (293 K), doublet peaks were observed corresponding to Zr 3d$_{5/2}$ and Zr 3d$_{3/2}$ centered at 181.9 eV and 184.3 eV, respectively. The doublet peaks were separated by 2.4 eV. the magnitude of spin-orbit splitting constant of Zr 3d. After the substrate heated to 623 K, the binding energies for Zr 3d$_{5/2}$ and 3d$_{3/2}$ were shifted to higher energy region about 0.2 eV to 182.1 and 184.5 eV from the peaks obtained zirconium oxide films formed at 293 K.[28] The peak shift to higher binding energy implies that the oxidation state of zirconium is increased. It may be due to the higher portion of zirconia (ZrO$_2$) than that of zirconium oxides (ZrO$_{x,y}$, x,y < 2. higher and lower oxidation states) as the substrate temperature increased. This could be explained by considering complete oxidation of zirconium with lower oxidation state to zirconia in its +4 oxidation state.[27,29,31]

To get more chemical information. peak deconvoultion process was performed. The representative deconvoluted high resolution XP spectra of the Zr 3d at 293 and 623 K are shown in Figures 5 (b) and (c). respectively. The Zr 3d spectra can be curve-fitted with three peaks: zirconia (ZrO$_2$), zirconium oxides with higher (ZrO$_x$: 0 < x < 2). and lower oxidation state (ZrO$_y$: 0 < y < 2. x > y).[32] The Zr 3d$_{5/2}$ of zirconia is centered at 182.1 eV, the Zr 3d$_{5/2}$ with higher oxidation state is centered at 182 eV, and the Zr 3d$_{5/2}$ with lower oxidation state is centered at 181.5 eV. As increased substrate temperature. the portion of zirconium oxide species with higher and lower oxidation state (ZrO$_{x,y}$) were decreased and that of zirconia (ZrO$_2$) species was increased. According to these results, we could confirmed that the higher substrate temperature caused more zirconia formation than zirconium oxides (ZrO$_{x,y}$) formation in the deposited thin films. The diffusion of oxygen through the zirconium oxide films was enhanced under high deposition temperature and formed fully oxidized zirconium species (zirconia). as zirconium oxide films have been previously reported to be an oxygen ion conductor and have high oxygen diffusivity.[33]

The representative O 1s XP spectra of zirconium oxide thin films on silicon substrate at different substrate temperatures were stacked in Figure 6 (a). Before zirconium oxide deposited on the silicon wafer. the O 1s peak of silicon dioxide (O-Si) strongly appeared at 531.7 eV.[26] After zirconium oxide deposited on Si(100). the O 1s peak of zirconium oxides (ZrO$_{x,y}$ and ZrO$_2$)

Figure 6. (a) O 1s region XP spectra of the zirconium oxide thin films on Si(100) with different substrate heating temperatures. The silicon dioxide (SiO₂) peak was centered at 531.7 eV, and the zirconium oxides (O-Zr) was assigned at 529.6 eV. Deconvoluted XP spectra of the O 1s at the silicon substrate temperature was 293 K (b) and 623 K (c). The O 1s spectra were deconvoluted four oxidation states: zirconia (ZrO₂), higher and lower oxidation states (ZrO$_{x,y}$), surface oxygen (O-surf), silicon dioxide (O-Si). The bottom solid lines are subtracted background by Shirley mode.
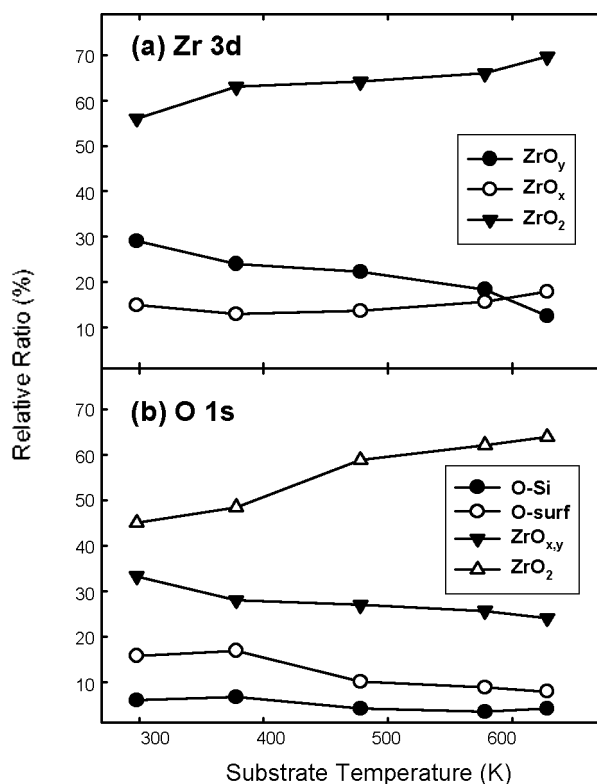
Figure 7. The relative peak area ratios of the Zr 3d (a) and O 1s (b) of the zirconium oxide thin films on Si(100) as a function of substrate temperatures.

peaks increased at 529.6 eV^{34} while that of O-Si decreased significantly. As increasing the substrate temperature. O 1s peak intensity was seemingly increased and this will be discussed later. Comparison with Figure 5 (a), the peak position of O 1s

Table 1. Average binding energy (BE) and full width at half maximum (FWHM) values applied in the deconvolution process; Zr 3d and O 1s components, as resolved from the measured Zr 3d and O 1s XPS spectra of zirconium oxide thin films on Si(100) substrate.

| Component	BE (eV)	FWHM (eV)
Zr 3d components		
Lower oxidation state (ZrO$_y$)	181.55 ± 0.17	1.08 ± 0.08
Higher oxidation state (ZrO$_x$)	182.00 ± 0.15	1.20 ± 0.10
Zirconia (ZrO₂)	182.15 ± 0.13	1.17 ± 0.09
O 1s components		
Zirconia (ZrO₂)	529.54 ± 0.19	1.37 ± 0.01
Higher and lower oxidation state (ZrO$_{x,y}$)	530.00 ± 0.06	1.62 ± 0.03
Surface oxygen (O-surf)	531.70 ± 0.12	1.42 ± 0.01
Silicon dioxide (O-Si)	532.41 ± 0.06	1.39 ± 0.02

shifted to higher binding energy about 0.2 eV. The shift of peaks Zr 3d and O 1s signifies that those oxidation states were changed. For the heating the Si substrate during zirconium oxide thin films deposition may cause partial bonding of zirconium atoms with the oxygen. The peak deconvolution was performed to get detail information and shown in Figures 6 (b) and (c).

The representative high resolution XP spectra of the O 1s region at 293 and 623 K are shown in Figures 6 (b) and (c), respectively. The O 1s spectra were decomposed with four peaks after the deconvoulution process; zirconium oxide (ZrO₂), higher and lower oxidation states of zirconium (ZrO$_{x,y}$), surface oxygen (O-surf), and silicon dioxide (O-Si). The O 1s peak of silicon dioxide (SiO₂) is centered at 532.4 eV. surface oxygen is centered at 531.7 eV. higher and lower oxidation state (ZrO$_{x,y}$) is centered at 530 eV. and zirconia (ZrO₂) is centered at 529.5 eV. The best fitting parameters used in the deconvolution processes are given in Table 1. The zirconium with higher and lower oxidation state was altered to the zirconia by increasing substrate temperature. The oxidation state of zirconium was changed and the zirconium oxide was stabilized on silicon substrate by increasing substrate temperature.

The integrated area ratios of Zr 3d and O 1s in different chemical environments with different substrate temperatures are shown Figures 7 (a) and (b), respectively. This showed zirconium oxides in higher and lower oxidation states (denoted as ZrO$_x$ and ZrO$_y$. respectively) changed to the zirconia (ZrO₂) as increasing substrate temperature. This consequence was well consistent with the XP spectra of Zr 3d and O 1s.

Figure 8 shows the valence band region XP spectra of zirconium oxide thin films coated on Si(100). The silicon substrate valence band spectra were dominated mainly by the Si 3s and Si 3p orbitals extending approximately 7 eV and from 4.5 to 1.5 eV. respectively.^{35} When the zirconium oxide deposited on silicon substrate, the valence band spectra were observed at around 4.5 to 7 eV.^{36,37} This valence band could be assigned to surface zirconium oxide which was overlapped with Zr 4d (6.7 eV) and O 2p (5 eV) orbitals.^{21,38}

The valence band maximum (VBM) values with different substrate temperatures are shown in Table 2. In each of the spectra, the VBM was determined by extrapolating the segment after applying linear least squares method. It is considered to the data obtained in this way, as increasing the substrate temperature
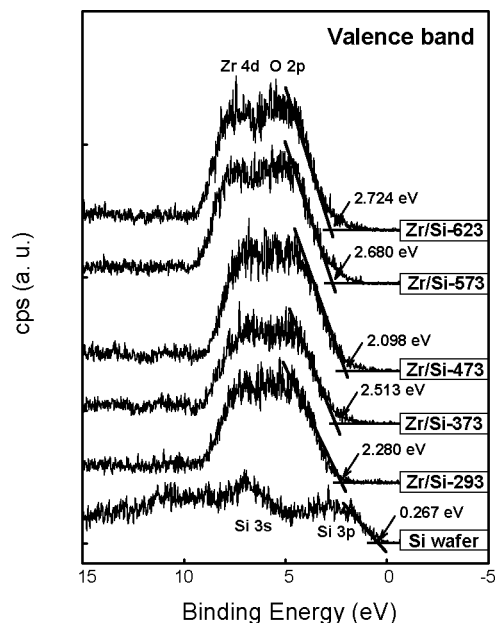
Figure 8. Valence band spectra for deposited zirconium oxide thin films on Si(100) with increased substrate temperature. The solid lines are extrapolating lines applying the least square method and the intersection of the solid lines represents the valence band maximum.

Table 2. The valence band maximum (VBM) according to the silicon substrate temperature

Substrate Temperature (K)	VBM (eV)
293	2.280
373	2.513
473	2.098
573	2.680
623	2.724

was increasing the valence band maximum. At the substrate temperature of 473 K. however. the VBM was decreased. This result was supported by XPS result explained it previously XP spectra of the Zr 3d and O 1s was indicated that peaks was shifted to lower binding energy substrate temperature at 473 K. This result shows that Zr-Si interface signal was appeared to lower binding energy.[39] It could be estimated that thickness of zirconium oxide thin film was comparative thinner than others.

Conclusions

Zirconium oxide thin films were deposited on p-type Si(100) with different substrate temperature in Ar/O_2 (1:1) plasma mixture applying radio frequency (RF) magnetron sputtering process. The zirconium oxide thin films surfaces were characterized by X-ray photoelectron spectroscopy (XPS), X-ray diffraction (XRD). Atomic Force Microscopy (AFM). and spectroscopic ellipsometry (SE) techniques.

The XPS confirmed that the change ZrO_x. ZrO_y (zirconium with higher and lower oxidation states) to ZrO_2 with increasing the substrate temperature. The XRD indicates the zirconium oxide forms a monoclinic crystal at 578 K. The AFM image

shows the roughness decreased by increasing the substrate temperature. The surface of thickness was comparative constant obtained by SE.

References

1. Venkataraj, S.; Kappertz, O.; Weis, H.; Drese, R.; Jayavel, R.; Wuttig, M. *J. Appl. Phys.* **2002**, *92*, 3599.
2. Gao, P. T.; Meng, L. J.; Snatos, M. P.; Teixeria, V.; Andritschky, M. *Vacuum* **2000**, *56*, 143.
3. Ma, C. Y.; Lapostolle, F.; Briois, P.; Zhang, Q. Y. *Appl. Surf. Sci.* **2007**, *53*, 8718.
4. Larsson, A. L.; Niklasson, A. G. *Sol. Energy Mater. Sol. Cells* **2004**, *84*, 351.
5. Baertsch, C. D.; Jensen, K. F.; Hertz, J. L.; Tuller, H. L.; Vengallatore, S. T.; Spearing, S. M.; Schmidt, M. A. *J. Mater. Res.* **2004**, *19*, 2604.
6. Lin, C.-Y.; Wu, C.-Y.; Wu, C.-Y.; Lin, C.-C.; Tseng, T.-Y. *Thin Solid Films* **2007**, *516*, 444.
7. Minh, N. Q. *J. Am. Ceram. Soc.* **1993**, *76*, 563.
8. Feldman, A.; Yang, X.; Farabaugh, E. N. *Appl. Opt.* **1989**, *28*, 5229.
9. Kuo, D. H.; Chen, C. H. *Thin Solid Film* **2003**, *429*, 40.
10. He, G.; Fang, Q.; Liu, M.; Zhu, L. Q.; Zhang, L. D. *J. Cryst. Growth* **2004**, *268*, 155.
11. Howard, J. M.; Cracium, V.; Essary, V.; Singh, R. K. *Appl. Phys. Lett.* **2002**, *81*, 3431.
12. Zhu, L. Q.; He, G.; Liu, M.; Fang, Q.; Zhang, L. D. *Mater. Lett.* **2006**, *60*, 888.
13. Wada, K.; Yamaguchi, N.; Matsubara, H. *Surf. Coat. Technol.* **2004**, *184*, 55.
14. Jeong, J.; Yong, K. *J. Cryst. Growth* **2003**, *254*, 65.
15. Carcia, P. F.; McLean, R. S.; Reilly, M. H.; Li, Z. G.; Pillione, L. J.; Messier, R. F. *J. Vac. Sci. Technol. A* **2003**, *21*, 745.
16. Pulker, H. K. *Surf. Coat. Technol.* **1999**, *112*, 250.
17. Wang, L. S.; Barnett, S. A. *J. Electrochem. Soc.* **1992**, *139*, 1134.
18. Huy, L. D.; Laffez, P.; Daniel, P.; Jouanneaux, A.; Khoi, N. T.; Siméone, D. *Mater. Sci. Eng. B* **2003**, *104*, 163.
19. JCPDS Database, International Center for Diffraction Data. **2003**, PDF 83-0940.
20. Kwon, J. H.; Youn, S. W.; Kang, Y.-C. *Bull. Korean Chem. Soc.* **2006**, *27*, 1851.
21. Jung, H. Y.; Kang, Y.-C. *Bull. Korean Chem. Soc.* **2007**, *28*, 1751.
22. Espitia-Cabrera, I.; Orozco-Hernandez, H. D.; Bartolo-Perez, P.; Contreras-Garcia, M. E. *Surf. Coat. Technol.* **2008**, *203*, 211.
23. Proceedings of *the International Conference Zirconia '88: Advances in Zirconia Science and Technology*, Meriani, S., Ed.; New York: Elesvier, 1989.
24. Venkataraj, S.; Kappertz, O.; Weis, H.; Drese, R.; Jayavel, R.; Wuttig, M. *J. Appl. Phys.* **2002**, *92*, 3599.
25. Zhu, L. Q.; Fang, Q.; Wang, X. J.; Zhang, J. P.; Liu, M.; He, G.; Zhang, L. D. *Appl. Sur. Sci.* **2008**, *254*, 5439.
26. *Handbook of X-ray Photoelectron Spectroscopy.* Wagner, C. D.; Riggs, W. M.; Davis, L. E.; Moulder, J. F.; Muilenberg, G. E., Eds.; Perkin-Elmer Corp.: Eden Prairie, MN, 1992; p 100.
27. Sun, Y.-M.; Lozano, J.; Ho, H.; Park, H. J.; Veldman, S.; White, J. M. *Appl. Surf. Sci.* **2000**, *161*, 115.
28. Cabillo, G.; Lillo, L.; Caro, C.; Buono-Core, G. E.; Chornik, B.; Soto, M. A. *J. Non-Cryst. Solids* **2008**, *354*, 3919.
29. Zhang, N. L.; Song, Z. T.; Wan, Q.; Shen, Q. W.; Lin, C. L. *Appl. Surf. Sci.* **2002**, *202*, 126.
30. Ohtsu, Y.; Ehami, M.; Fujita, H.; Yukimura, K. *Surf. Coat. Technol.* **2005**, *196*, 81.
31. Jeon, T. S.; White, J. M.; Kwong, D. L. *Appl. Phys. Lett.* **2001**,

78, 368.

32. Qi, W.-J.; Nieh, R.; Lee, B. H.; Kang, L.; Jeon, Y.; Lee, J. C. *Appl. Phys. Lett.* **2000**, *77*, 3269.

33. He, G.; Fang, Q.; Zhang, J. X.; Zhu, L. Q.; Liu, M.; Zhang, L. D. *Nanotechnology* **2005**, *16*, 1647.

34. Zhu, L. Q.; Fang, Q.; He, G.; Liu, M.; Xu, X. X.; Zhang, L. D. *Mater. Sci. Semicond. Pro.* **2006**, *9*, 1025.

35. Tolinski, T.; Kowalczyk, A.; Chelkowska, G.; Mihalik, M.; Tinko, M. *Act. Phys. Polonica A* **2008**, *113*, 1.

36. Miyazaki, S.; Narasaki, M.; Ogasawara, M.; Hirose, M. *Microelectron. Eng.* **2001**, *59*, 373.

37. Miyazaki, S.; Narasaki, M.; Ogasawara, M.; Hirose, M. *Solid-State Electronics* **2002**, *46*, 1679.

38. Crist, B. V. *Handbook of Monochromatic XPS Spectra: The Elements and Native Oxides*. John wiley & Sons Ltd: Baffins Lane, Chichester, West Sussex PO19 1UD, England, 2000; p 515.

39. Chua, D. H. C.; Milne, W. I.; Zhao, Z. W.; Tay, B. K.; Lau, S. P.; Carney, T.; White, R. G. *J. Non-Cryst. Solids* **2008**, *332*, 185.